

See discussions, stats, and author profiles for this publication at: <https://www.researchgate.net/publication/236238898>

# A Coding Technique with Progressive Reconstruction Based VQ and Entropy Coding Applied to Medical Images

Conference Paper in Proceedings of SPIE - The International Society for Optical Engineering · August 2000

DOI: 10.1117/12.411600

CITATIONS

0

READS

50

4 authors, including:



**Marcos Martin-Fernandez**  
Universidad de Valladolid

172 PUBLICATIONS 1,342 CITATIONS

[SEE PROFILE](#)



**Carlos Alberola-López**  
Universidad de Valladolid

240 PUBLICATIONS 2,833 CITATIONS

[SEE PROFILE](#)



**Juan Ruiz-Alzola**  
Universidad de Las Palmas de Gran Canaria

94 PUBLICATIONS 1,229 CITATIONS

[SEE PROFILE](#)

Some of the authors of this publication are also working on these related projects:



Resonancia magnética cardíaca isotrópica de cine y extensión a angiografía sin contraste: reconstrucción 100% eficiente mediante muestreo compresivo y estimación conjunta de movimiento cardio-respiratorio [View project](#)



DynamicREC: High resolution 100% efficient dynamic magnetic resonance image reconstruction: solutions based on advanced 5D image processing and machine learning paradigms [View project](#)

# A Coding Technique with Progressive Reconstruction Based on VQ and Entropy Coding Applied to Medical Images

Marcos Martín-Fernández<sup>§</sup>, C. Alberola-López<sup>§</sup>, D. Guerrero-Rodríguez<sup>§</sup>, and J. Ruiz-Alzola<sup>‡</sup>

<sup>§</sup>ETSI Telecomunicación. Universidad de Valladolid, Spain.

<sup>‡</sup>ETSI Telecomunicación. Universidad de las Palmas de Gran Canaria, Spain.

## ABSTRACT

In this paper we propose a novel lossless coding scheme for medical images that allows the final user to switch between a lossy and a lossless mode. This is done by means of a progressive reconstruction philosophy (which can be interrupted at will) so we believe that our scheme gives a way to trade off between the accuracy needed for medical diagnosis and the information reduction needed for storage and transmission.

We combine vector quantization, run-length bit plane and entropy coding. Specifically, the first step is a vector quantization procedure; the centroid codes are Huffman-coded making use of a set of probabilities that are calculated in the learning phase. The image is reconstructed at the coder in order to obtain the error image; this second image is divided in bit planes, which are then run-length and Huffman coded. An second statistical analysis is performed during the the learning phase to obtain the parameters needed in this final stage.

Our coder is currently trained for hand-radiographs and fetal echographies. We compare our results for this two types of images to classical results on bit plane coding and the JPEG standard. Our coder turns out to outperform both of them.

**Keywords:** Vector Quantization, Entropy Coding, Progressive Reconstruction, Run-length, Bit Planes, Radiographies, Echographies

## 1. INTRODUCTION

Graphical information exchange is nowadays common practice due to the current capabilities of network communications and graphical terminals; as equipments get ready for more involved graphical applications the end-user requires faster access to databases, interactivity and so forth. Quite a few applications areas require naturality and interactivity and some of them are, undoubtedly, those classified with the word telemedicine.

Networked applications involving health care are particularly resource demanding; on one side, issues like naturality in the communication between the patient and the physicist, fast information retrieval from medical databases, and rapid browsing in graphical files are compulsory. On the other, the storage needs grow unboundedly due to the ubiquity of imaging devices: MRI, CAT, ultrasound and others. These two trends make compression schemes a necessary tool to achieve a satisfactory trade-off between the two aspects of the problem.

In this paper we propose a compression scheme which is based on state-of-the-art ideas that have been properly selected, and put together and trained for two specific types of medical images, namely, radiographs and echographies. We have obtained interesting results that allow us to compare different learning strategies for vector quantization; in addition, we propose rigorous methods to learn probabilities from the data used in the training stage.

The paper is structured as follows: in Section 2 we start with a background which is intended to make the paper self contained. Section 3 describes and justifies the coder-decoder structure. Finally, Section 4 describes the experiments we have done to quantify the coded performance.

## 2. BACKGROUND

As we just said, no new ideas are given in this section. Apart from the specific references given in the subsection on vector quantization, the material in this section can be found in classical textbooks<sup>1,2</sup>

---

Correspondence should be addressed to Marcos Martín at ETSIT Telecomunicación, Universidad de Valladolid, Campus Miguel Delibes, s/n, 47011 Valladolid, Spain or at marcos.martin@tel.uva.es.

## 2.1. Vector Quantization

Vector quantization is the natural extension to multiple dimensions of the scalar quantization. It can be easily demonstrated<sup>2</sup> that in those cases where the image data are correlated, vector quantization shows a lower bit rate at the same level of distortion than scalar quantization or, conversely, a smaller distortion is achieved at the same bit rate.

Vector quantization first extract blocks of pixels from the original image and quantize them as a whole. Specifically, denoting by  $Y = [y_1, y_2, \dots, y_k]$  a vector of  $k$  pixel values extracted from the original image, the vector quantization is a *many-to-one* correspondence defined as

$$Y \rightarrow \hat{Y}_i \quad \text{if } Y = [y_1, y_2, \dots, y_k] \in C_i \quad i = 1, \dots, N_c \quad (1)$$

with  $\hat{Y}_i = [\hat{y}_{i1}, \hat{y}_{i2}, \dots, \hat{y}_{ik}]$  the  $i$ -th quantization point in the original space  $\mathfrak{R}^k$  and  $N_c$  the number of allowed quantization points; quantization points are called *centroids* and the set of centroids is called the *codebook*. Finally,  $C_i$  is the region of influence of the  $i$ -th centroid, i.e., the region in the original space  $\mathfrak{R}^k$  where all the vector lying in that region are quantized (or clustered) to the  $i$ -th centroid. It is customary that  $N_c$  is a power of two, i.e.,  $N_c = 2^b$  so each centroid can be addressed with a binary code of  $b$  bits.

The complexity in the vector quantization procedure grows linearly with  $N_c$  and exponentially with the block dimension  $k$ . Therefore, too large a dimension for the blocks is not advisable. Moreover, the larger the blocks the more perceivable the *blocking effect* in the quantized reconstructed image. On the other hand, if blocks are too small, the block may not fully capture the correlation within the data and consequently most of the advantages of the vector quantization would be lost. Typical dimensions for the selected blocks are  $4 \times 4$  or  $8 \times 8$ .

How the  $N_c$  centroids are chosen for a set of images is an important issue in vector quantization. This is typically done by means of a training phase, in which the position of the centroids  $\hat{Y}_i$  is selected out of  $T$  training vectors  $Y_t$ ,  $t = 1, \dots, T$ . It is clear that the training set should be representative of the population that is going to be quantized, and the number  $T$  should be as large as possible.

In this paper we will use three training methods. The first of them is the well known *K-means* or *LBG* algorithm.<sup>3</sup> This algorithm is a recursive procedure based on the following ideas:

- Assume that at the  $n$ -th step of the algorithm we have the  $N_c$  tentative centroids  $\hat{Y}_i(n)$  (Initially, i.e., at  $n = 0$ , the first set of centroids can be chosen arbitrarily, although more elaborated versions exist<sup>3</sup>).
- The vectors in the training set  $Y_t$ ,  $t = 1, \dots, T$  are assigned to the closer tentative centroid (in some metric, typically the classical Euclidean distance is used).
- Those training vectors assigned to the tentative centroid  $\hat{Y}_i(n)$  are used to recalculate the new position  $\hat{Y}_i(n+1)$  of this centroid, as the center of gravity of the vectors in this cluster.

The process continues until the change in average distortion (or, equivalently, the change in the centroids position) are below some prespecified threshold.

This algorithm depends strongly on the initial set of tentative centroids. To overcome this problem, other procedures have been proposed. Competitive learning (hereon CL)<sup>4</sup> is one of them. In this type of learning the distance of every vector  $Y_t$  in the training set to every tentative centroid is compared. The centroid closer (say, the  $i$ -th centroid) to this training vector is slightly modified according to the following rule

$$\hat{Y}_i(t, n-1) = \hat{Y}_i(t-1, n-1) + \eta(n) \left( Y_t - \hat{Y}_i(t-1, n-1) \right) \quad (2)$$

with  $\eta(n)$  a decaying exponential with  $n$  and  $\hat{Y}_i(t-1, n-1)$  the position of the  $i$ -th centroid after the  $t-1$  training sample has been considered at the  $(n-1)$ -th iteration of the algorithm. This means that, for every sample in the training set, only the centroid closer to this sample is modified (and moved closer to the training sample), while the others stand still ( $\hat{Y}_j(t, n-1) = \hat{Y}_j(t-1, n-1)$  with  $j \neq i$ ). The rate of motion of every tentative centroid shrinks as the iterative algorithm progresses.

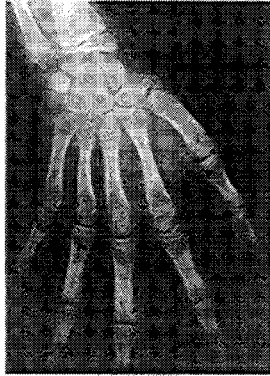


Figure 1. A hand radiograph in the data base.

This algorithm has been shown<sup>5</sup> to be an adaptive version of the LBG training method, so a fairly close performance to LBG should be expected, and only in very special cases this second philosophy shows a better behavior. However, the algorithm can be improved by a selection method based on the *equidistortion principle*, which reads<sup>5</sup>:

*For a large number of representative vectors, even though the underlying probability distribution of the input vector consists of multiple disjoint clusters, every partitioned region should have the same subdistortion for minimizing the expected distortion.*

Based on this idea, the distortion associated to every tentative cluster  $\hat{Y}_i(T, n)$  is calculated after the  $T$  training samples have been considered. For those clusters whose associated distortions are large, more centroids should be assigned, while those clusters with a very small distortion can be eliminated (so that the overall number of centroids is  $N_c$ ). The detailed calculation of how many more centroids should be assigned to a specific cluster is done on the basis of relative distortions between clusters. Of paramount importance is how this number changes with the iteration step. As it is customary, the number of centroids that are modified gets smaller with the iteration index. An example of such a function is  $s(n) = 2 \left\lceil \frac{s(0) \exp(-0.5n)}{2} \right\rceil$ . Typically  $s(0) = N_c/8$ . If  $s(0) = 0$ , no selection is made, and the learning is only a CL procedure. CL with the selection method will be hereon referred to as CL+SEL.

## 2.2. Bit Plane Encoding

Bit plane encoding (BPE) is based on splitting the original  $p$ -bit-per-pixel image into  $p$  images of the same size that the original, but with one bit per pixel. An example of such a split applied to the original image in figure 1 is shown in figure 2. It is clear from the example that the images from the most significant planes (upper row in figure 2) contain the information of the structure in the original image, while the less significant plane add the details, but the appearance is noisier.

BPE allows a simple procedure for progressive transmission and representation. For rapid browsing, only two or three of the most representative planes may suffice.

## 2.3. Run-length Encoding

Run-length encoding (RLE) is a widely-used procedure to encode one-bit images. This type of codification only codes the image dimensions, the first bit (whether 0 or 1) and the length of the alternate runs of 0's and 1's. As a rule, a run of 1's will be followed by a run of 0's and so forth. However, since the maximum codeable run size has to be binary coded, one might encounter cases in which a run exceeds this number; in this case the coding has to have a way to encode the possibility that a run of a digit is followed by one or more runs of the same digit. Also, a second special symbol meaning *end of image* is needed. Therefore, if we denote by  $K$  the maximum allowable run size, the number  $N_r$  of bits per run-length symbol is related to  $K$  by  $2^{N_r} = K + 2$ .

The optimum value of  $K$  is a trade off between two concepts. Too large a  $K$  would encode short runs with an unnecessary large binary word. However, too short a  $K$  requires a large number of non-alternance symbols. In our case, we have calculated the optimum value of  $K$  by analyzing the histograms of the run-length symbols from the set of training images.

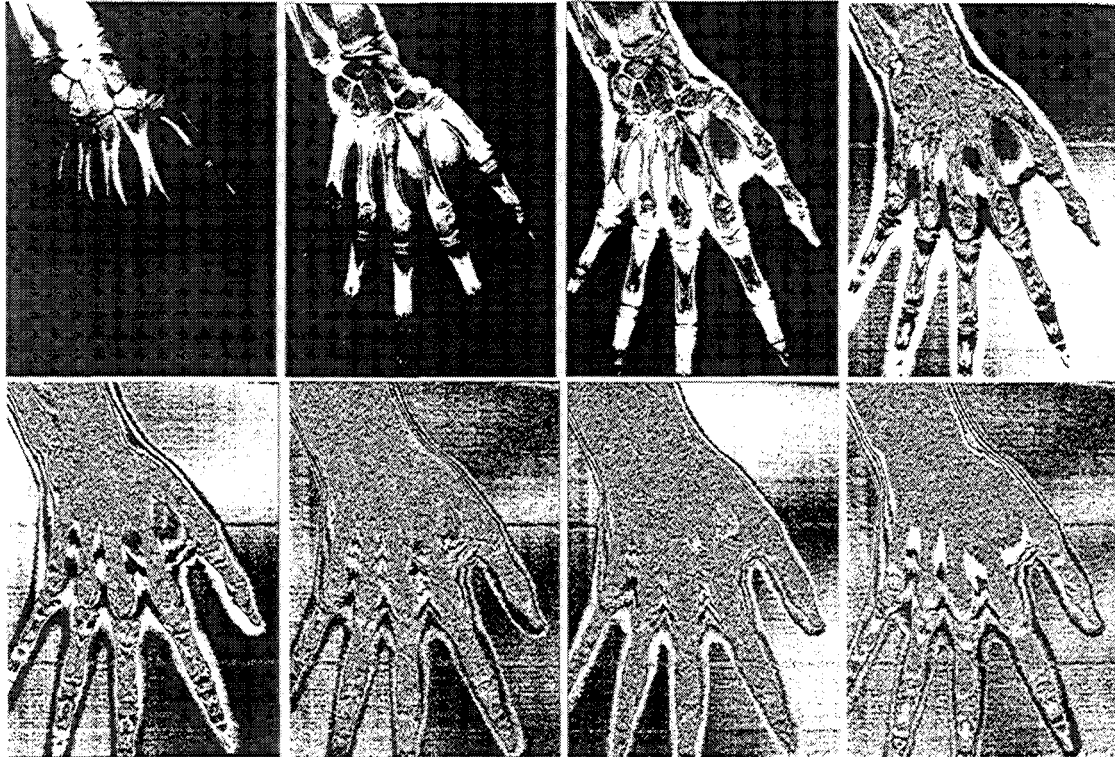


**Figure 2.** Bit planes of the radiograph in figure 1. The MSB plane is the upper-left image. THE LSB is the lower-right image.

### 2.4. Huffman Coding

As the Shannon theorem says, a source with  $L$  symbols  $s_i$ , each of them with a probability  $p(s_i)$ , has an entropy

$$H = - \sum_i p(s_i) \log_2 p(s_i). \quad (3)$$

and, ideally, could be coded with  $H$  bits. If all the symbols in the source are equiprobable, and  $L = 2^{N_r}$ , then the optimum code is a fixed-length code of  $N_r$  symbols. However, in real cases, the symbols show different probabilities, so variable-length codes are usually more efficient (in terms of less average bits per pixel than fixed-length codes) than fixed-length codes.

The most efficient realizable code was proposed long ago by Huffman<sup>6</sup>; he devised a constructive procedure to get such a code, which turns out to be uniquely decipherable as well. All that is needed is an estimate of the probabilities of the symbols in the source. We have made extensive use of this procedure with two different sources.

### 3. THE CODEC

Figures 3 and 4 show respectively the coder and decoder block diagrams. We will make use of them throughout the section. This codec will be denoted by VQBPC.

With respect to the coder, the upper branch in figure 3 carries out a vector quantization procedure. The original image is divided into square  $k$ -pixels blocks ( $k = l \times l$ ), which are reorganized as vectors; the codebook is searched to find the quantized value  $\hat{Y}_i$  for every vector. Note that the only information that needs to be stored is the index  $i$  of the centroid to which every input vector is quantized. The whole set of indexes is then Huffman coded. As it can be inferred, the training phase has incorporated a procedure to find out the probabilities of the centroids' indexes.

The middle and lower branches represent the second procedure performed by the coder. The quantized vectors  $\hat{Y}_j$  are reorganized as blocks, and the quantized image is reconstructed; this image is subtracted from the original

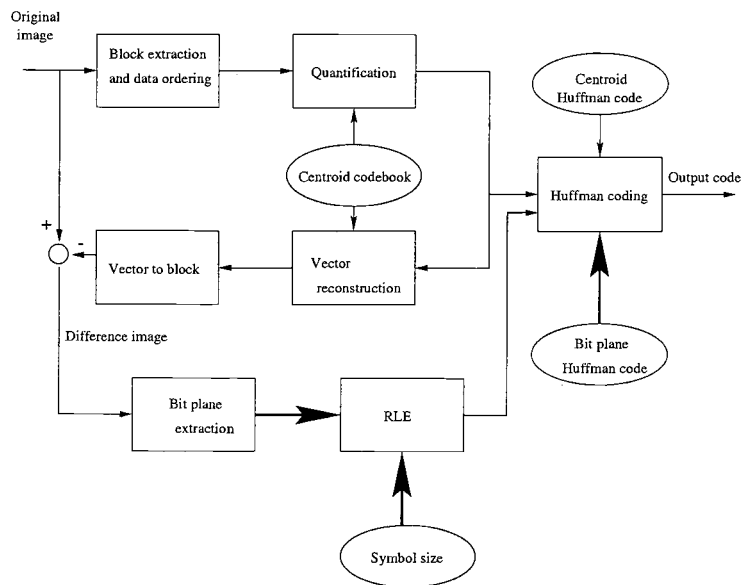


Figure 3. Coder block diagram.

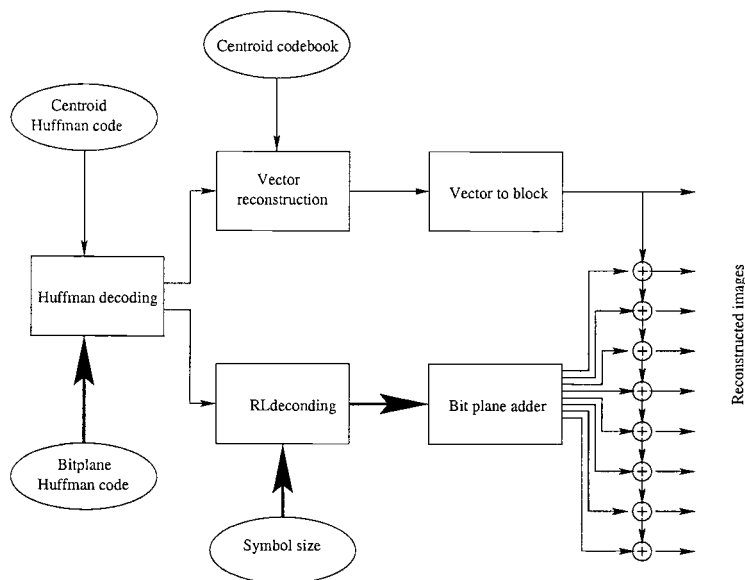


Figure 4. Decoder block diagram.

image, and the resulting image, i.e., the difference image, is divided into  $p$  bit planes plus the sign plane. Each of these  $p + 1$  images are run-length coded, and finally, the run-length symbols of every image are Huffman coded.

Therefore, the resulting frame is:

1. The original image dimensions ( $M$  rows times  $N$  columns, since this information is lost after the block extraction procedure).
2. Huffman coded centroid indexes.
3. For each of the  $p + 1$  one-bit images, a first bit to indicate whether we start with a 0 or a 1; then the Huffman-coded run-length symbols.

The decoder structure is shown in figure 4; once the image dimensions and the Huffman-coded centroid indexes have been received, the vector quantized image  $\tilde{Y}_j$  can be reconstructed, so the first lossy version of the image is created in the upper branch of the block diagram; then, each of the bit planes can be decoded and added to the reconstructed image, so a progressive reconstruction can be obtained and the procedure can be interrupted at will. When the  $p + 1$  bit planes are received and added, the original image is perfectly reconstructed.

Both the coder and the decoder make use of a number of libraries (represented in both block diagrams as ellipses) which have to be computed beforehand. The libraries are:

1. The vector quantization centroids. They are determined from a set on training images and stored. Note that the training phase has to be done once, and it is an off-line procedure. At present, we have implemented the methods we have described in section 2.1, namely, LBG, CL and CL+SEL.
2. When these training images are vector quantized, we obtain quite a few centroid indexes which can be used to estimate the relative frequencies of each centroid index. This information is used to build the Huffman code of centroid indexes.
3. Additionally, for each of the images in the training set, we compute the difference image and split it into its bit planes; once again, these images are used to estimate the histogram of the run-lengths of both 0's and 1's, as an intermediate step to find the optimum values of  $K$  and  $N_r$  for every bit plane. A further piece of information to be considered is the fact that Huffman codes for  $N_r > 11$  is highly inefficient.
4. Finally, and as we did for the centroid indexes, the relative frequencies of the run-length symbols are computed, and input into the Huffman tables for each bit plane.

As a summary, the parameters are: the centroids and their Huffman codes, the  $p + 1$  lengths of the run-length symbols and the  $p + 1$  Huffman codes of these symbols.

For the sake of comparison we have also trained a similar codec without the vector quantization stage, but only with the bit plane operative. This coding technique will be denoted by BPCO (bit plane coding only). Comparative results will be shown in the following section.

#### 4. EXPERIMENTS

The codec has been trained both for a set of hand radiographs,<sup>7</sup> and also for a volume data set of a fetal echography which has been used elsewhere.<sup>8</sup> For the sake of brevity, we only give details of the codec parameters for the radiograph data set:

- $p = 8$  bits-per-pixel, i.e., 256 gray-level images. The data set consists of ten images.
- For BPCO the defining parameters are shown in table 1. The corresponding run-length parameters for the VQBPC are shown in table 2.
- For vector quantization, the number of centroids is  $N_c = 256$ , the number of training vectors is  $T = 68780$  and the vector length is  $k = 16$  ( $l = 4$ ). With this parameter set, the compression rate if Huffman code were not used would be  $kp/b = 16$ , with  $b = \log_2 N_c = 8$ .

	plane 7	plane 6	plane 5	plane 4	plane 3	plane 2	plane 1	plane 0
$K$	2046	1022	510	510	510	510	1022	510
$N_c$	11	10	9	9	9	9	10	9

**Table 1.** Parameters of the BPCO.

	plane sign	plane 7	plane 6	plane 5	plane 4	plane 3	plane 2	plane 1	plane 0
$K$	254	2	2046	2046	2046	2046	1022	254	510
$N_c$	8	2	11	11	11	11	10	8	9

**Table 2.** Run-length parameters for the difference image in the VQBPC.

The quality of the coding method will be quantitatively studied according to the following parameters:

1. Mean square error, i.e., the energy in the error image:

$$\langle e^2 \rangle = \frac{1}{MN} \sum_{M,N} (y[x_1, x_2] - \hat{y}[x_1, x_2])^2 \quad (4)$$

2. Mean absolute value of the difference image:

$$\langle |e| \rangle = \frac{1}{MN} \sum_{M,N} \text{abs}(y[x_1, x_2] - \hat{y}[x_1, x_2]) \quad (5)$$

This value should be compared to the maximum gray level intensity in a 8-bit-image, i.e., the intensity value 255.

3. Logarithmic signal-to-noise ratio:

$$SNR = 10 \log_{10} \left( \frac{\frac{1}{MN} \sum_{M,N} y[x_1, x_2]^2}{\langle e^2 \rangle} \right) \quad (6)$$

4. Compression rate:

$$r = \frac{\text{Bits in original image}}{\text{Bits in compressed image}} \quad (7)$$

The experiments are the following:

- Hand radiographs with the BPCO. Table 3 shows the parameters we have just defined as more bit planes are added to the reconstructed image. It is clear that a high compression ratio is achieved with only one bit plane at the expense of a very low SNR. An acceptable subjective quality is achieved with 5 bit planes; the compression rate has lowered to 4:1. The lossless compression rate is as low as 1.68:1.
- Hand radiographs with VQBPC. Tables 4, 5 and 6 show the respective numerical results for the LBG, CL and CL+SEL training methods respectively. Figure 5 shows a detailed area (extracted from the image in figure 1) of the compressed image for different methods. See the caption for details.

When no bit planes are added, the tables show that LBG has a higher compression ratio (32 % higher than CL and 29.6 % higher than CL+SEL) with a SNR fairly equal to the others. We can conclude there seems to

	$\langle e^2 \rangle$	$\langle  e  \rangle$	SNR (dB)	$r$
1 plane	1962.633	33.463	3.190	76.211 : 1
2 planes	798.249	23.720	7.097	25.056 : 1
3 planes	288.917	15.297	11.510	11.889 : 1
4 planes	71.822	7.095	17.556	6.432 : 1
5 planes	15.139	3.197	24.317	4.007 : 1
6 planes	3.750	1.580	30.378	2.756 : 1
7 planes	0.507	0.507	39.072	2.125 : 1
8 planes	0	0	$\infty$	1.681 : 1

**Table 3.** Quantitative results for the BPCO for hand radiographs.

	$\langle e^2 \rangle$	$\langle  e  \rangle$	SNR (dB)	$r$
Quantized image	22.01	3.04	22.7	22.59 : 1
Quantized image + 1 plane	22.01	3.04	22.7	6.57 : 1
Quantized image + 2 planes	21.93	3.04	22.7	6.44 : 1
Quantized image + 3 planes	20.58	3.01	22.98	6.11 : 1
Quantized image + 4 planes	14.59	2.76	24.46	5.51 : 1
Quantized image + 5 planes	7.8	2.24	27.2	4.51 : 1
Quantized image + 6 planes	2.38	1.27	32.34	3.1 : 1
Quantized image + 7 planes	0.49	0.49	39.14	2.3 : 1
Quantized image + 8 planes	0	0	$\infty$	1.8 : 1

**Table 4.** Quantitative results for the VQBPC-LBG for hand radiographs.

be no reason to choose CL (with or without selection) as opposed to LBG. In addition, the time taken to train the codec is far longer with the former.

As more planes are added to the vector quantized image, the CL methods slightly overcome the LBG; for example, with 5 planes, the compression ratios are fairly equivalent, though the CL and CL+SEL lead in SNR with a gain higher than 1 dB with respect to LBG. In the lossless mode, compression ratios of the CL methods are higher, though the difference is not outstanding.

The VQBPC methods, however, show a higher performance than the BPCO; if the case of 5 planes is inspected we can see that the compression rates are higher in the former and with a higher quality in the reconstructed images. For the lossless case, the compression rates are also higher.

An important detail to highlight is the fact that adding the first two bit planes hardly improves the reconstructed image quality though the compression rate worsens rapidly. This is due to the small amount of information associated to these planes (most of the values are pretty close to zero) but the sign plane is needed to perform the arithmetics correctly, and the latter plane has a high informative content; such a content needs a non-negligible bit allocation, which is the responsible for the decay of the compression rate.

Finally, as far as the JPEG<sup>9</sup> is concerned, the two rightmost images in figure 5 show comparable compression ratios, though the image quality is much higher in the VQBPC with 5 bit planes than in the JPEG compressed. Specifically, the SNR for the VQBPC is 28.47 dB and the SNR for the JPEG turned out to be 25.57 dB. Although visually the difference is hard to notice, a close inspection reveals a grainier appearance in the JPEG image, along with several false contours; it is clear that JPEG works in a transformed domain, so the inverse transform performed on quantized coefficients introduces changes in the position of outstanding features; such changes if input into a pattern recognizer may lead to confusion.

	$\langle e^2 \rangle$	$\langle  e  \rangle$	$SNR$ (dB)	$r$
Quantized image	21.9	2.53	22.7	17.07 : 1
Quantized image + 1 plane	21.9	2.53	22.7	5.73 : 1
Quantized image + 2 planes	21.83	2.53	22.72	5.69 : 1
Quantized image + 3 planes	19.99	2.48	23.11	5.45 : 1
Quantized image + 4 planes	12.89	2.19	25.02	4.98 : 1
Quantized image + 5 planes	5.77	1.65	28.51	4.15 : 1
Quantized image + 6 planes	2.29	1.10	32.53	3.31 : 1
Quantized image + 7 planes	0.44	0.44	39.67	2.37 : 1
Quantized image + 8 planes	0	0	$\infty$	1.84 : 1

**Table 5.** Quantitative results for the VQBPC-CL for hand radiographs.

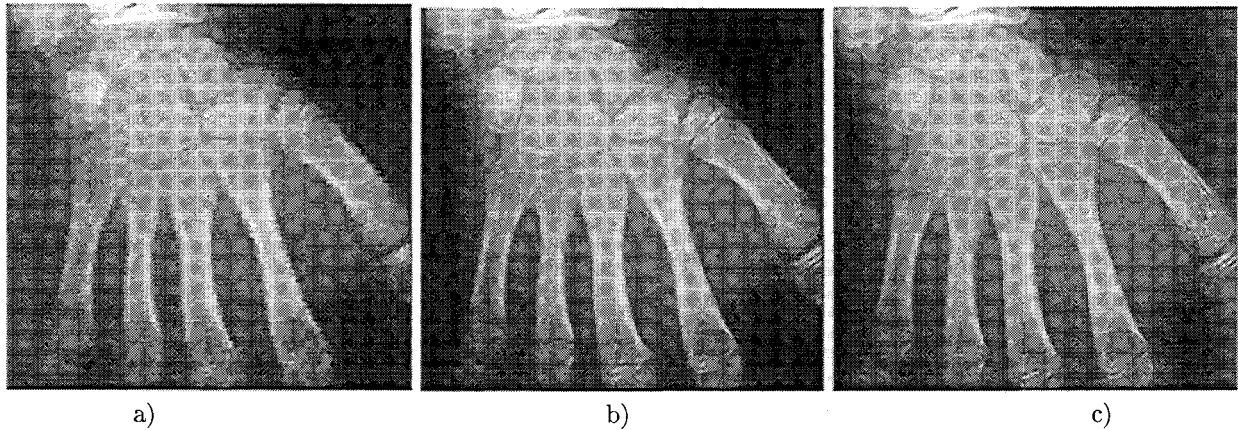


**Figure 5.** a) Compressed image with CL+SEL. No bit planes added. b) Compressed image with CL+SEL. 5 bit planes (plus sign) added. c) JPEG-compressed at a rate 4.28:1.

	$\langle e^2 \rangle$	$\langle  e  \rangle$	$SNR$ (dB)	$r$
Quantized image	21.188	2.508	22.857	17.433 : 1
Quantized image + 1 plane	21.188	2.508	22.857	5.785 : 1
Quantized image + 2 planes	21.159	2.507	22.863	5.739 : 1
Quantized image + 3 planes	19.3635	2.467	23.248	5.682 : 1
Quantized image + 4 planes	12.733	2.192	25.069	5.229 : 1
Quantized image + 5 planes	5.816	1.664	28.472	4.381 : 1
Quantized image + 6 planes	2.312	1.106	32.477	3.447 : 1
Quantized image + 7 planes	0.443	0.443	39.650	2.441 : 1
Quantized image + 8 planes	0	0	$\infty$	1.878 : 1

**Table 6.** Quantitative results for the VQBPC-CL+SEL for hand radiographs.

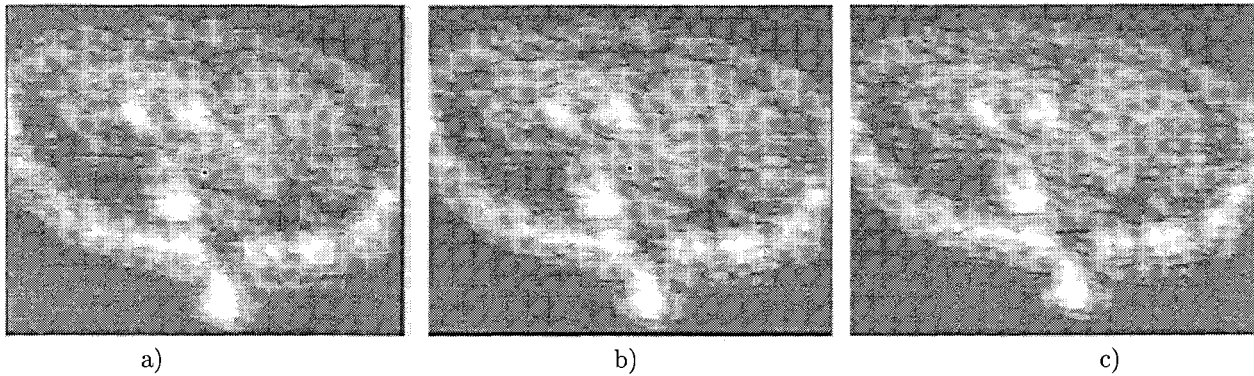


**Figure 6.** a) Compressed image with CL+SEL. No bit planes added. b) Compressed image with CL+SEL. 5 bit planes (plus sign) added. c) JPEG-compressed at a rate 4.96:1.

- Echographies with BPCO. Table 7 shows the quality results as more bit planes are added to the reconstructed image. The version with 5 planes attains acceptable levels of SNR. The compression rate is 4.18:1. The lossless version has a compression rate of 1.81:1.

	$E\{e^2\}$	$\langle e \rangle$	SNR (dB)	$r$
1 plane	5031.89878	61.603078	1.719967	75.004166 : 1
2 planes	395.729573	14.950521	12.857695	33.878946 : 1
3 planes	190.890208	11.692822	15.93556	18.246326 : 1
4 planes	101.779574	7.970005	18.825988	6.80601 : 1
5 planes	18.382788	3.352465	26.094831	4.187677 : 1
6 planes	2.764653	1.202614	34.320564	2.947168 : 1
7 planes	0.378839	0.378839	42.952404	2.243719 : 1
8 planes	0	0	$\infty$	1.811601 : 1

**Table 7.** Quantitative results for the BPCO for a fetal echography volume data set.

- Echographies with VQBPC-CL+SEL. Results are shown in table 8. Figure 5 shows a zoomed area of the head of a fetus compressed with different compression methods. See the caption for details. The quantized version has a quality of 25.85 dB and a compression rate of 19:1. As we said before, the addition of the most significant planes does not improve the image quality much. However, when the 5-th plane is added, a visually-lossless image is reconstructed (see figure 5). SNR grows to 32.38 dB and the compression rate lowers to 5.05:1. With respect to BPCO, quality is 61 % higher and the compression rate is 21 % larger. The lossless version compression rate is also higher in this case than in the BPCO.

If we now compare to JPEG (see the two rightmost images in figure 5), VQBPC with 5 planes has a compression 5.05:1 and the JPEG is 4.96:1: There is a clear difference in SNR, the VQBPC is 32.38 dB versus the 23.8 dB given by the JPEG. The same comments as before apply.

## 5. CONCLUDING REMARKS

In this paper we have presented a coding scheme that makes use of both vector quantization and bit plane coding methods to obtain a progressive reconstruction lossless coding scheme; the reconstruction can be interrupted at user's will, and, if so, the coding method will be lossy. We have carried out extensive data analysis to obtain the relative frequencies of all the symbols used by the two symbol sources built in our codec.

The experiments have shown the performance of the codec as a function of the number of bit planes used in the reconstruction. We have checked that, for the images considered, a reconstruction with 5 bit planes draws visually

	$E\{e^2\}$	$\langle e \rangle$	SNR (dB)	$r$
Quantized image	19.94409	2.150099	25.85637	19.015168 : 1
Quantized image + 1 plane	19.94409	2.150099	25.85637	6.6091183 : 1
Quantized image + 2 planes	19.94409	2.150099	25.85637	6.608983 : 1
Quantized image + 3 planes	18.45456	2.11478	26.19515	6.51697 : 1
Quantized image + 4 planes	11.356706	1.81804	28.32075	5.959835 : 1
Quantized image + 5 planes	4.41188	1.299266	32.3803656	5.0553 : 1
Quantized image + 6 planes	1.684571	0.87989	36.48368	4.13901 : 1
Quantized image + 7 planes	0.396499	0.396499	42.7545	2.962617 : 1
Quantized image + 8 planes	0	0	$\infty$	2.27683 : 1

**Table 8.** Quantitative results for the VQBPC-CL+SEL for a fetal echography volume data set.

lossless images. In all the cases, the whole scheme, i.e., the codec based on vector quantization and bit plane encoding, outperforms a codec based solely on bit plane encoding. Moreover, a comparison with the JPEG standard has also been carried out. For comparable compression ratios, the JPEG image shows a noisier subjective look; moreover, the quantitative differences in the qualities of the reconstructed images are clear.

#### ACKNOWLEDGMENTS

This paper has been partially supported by research grants TIC97-0772, VA78/99 and 1FD97-0881. The authors want to thank Prof. Yang at Saskatchewan University, Canada, for sharing with us the ultrasound data we have used in our research. Thanks are also due to Hospital de Medina del Campo for the radiographs data set.

#### REFERENCES

1. A. K. Jain, *Fundamentals of Digital Image Processing*, Prentice-Hall, New Jersey, 1989.
2. J. S. Lim, *Two-Dimensional Digital and Image Processing*, Prentice-Hall, New Jersey, 1990.
3. Y. Linde, A. Buzo, R. M. "Gray, An Algorithm for Vector Quantizer Design", *IEEE Trans. on COM*, **28**, pp. 84-95, 1980.
4. T. Kohonen, *Self-organization and associative memories*, Springer-Verlag, New York, 1984.
5. N. Ueda, R. Nakano, "A New Competitive Learning Approach Based on Equidistortion Principle for Designing Optimal Vector Quantizers," *Neural Networks*, **7**, pp. 1211-1227, 1994.
6. D. A. Huffman, "A Method for the Construction of Minimum-Redundancy Codes," *Proc. of the IRE*, **40**, pp. 1098-1101, 1952.
7. S. Wong, L. Zaremba, D. Gooden, H. K. Huang, "Radiologic Image Compression - A Review," *Proc. of the IEEE*, **83**, pp. 194-219, 1995.
8. N. Weng, Y. H. Yang and R. Pierson, "Three-Dimensional Surface Reconstruction Using Optical Flow for Medical Imaging," *IEEE Trans. On Medical Imaging*, vol. 16, no. 5, pp. 630-641, 1997.
9. G. K. Wallace, "The JPEG Still Picture Compression Standard," *Communications of the ACM*, **34**, pp. 30-44, 1991.